Physics in Medicine 1 (2016) 20–26

Contents lists available at ScienceDirect

Physics in Medicine

journal homepage: http://www.journals.elsevier.com/physics-in-medicine

Comparing the accuracy of master models based on digital intra-oral scanners with conventional plaster casts

Christoph Vögtlin, Georg Schulz*, Kurt Jäger, Bert Müller

Biomaterials Science Center, University of Basel, Gewerbestrasse 14, 4123 Allschwil, Switzerland

ARTICLE INFO

Article history:
Received 29 December 2015
Received in revised form
5 April 2016
Accepted 6 April 2016
Available online 13 April 2016

Keywords:
Oral scanner
Micro computed tomography
Three-dimensional non-rigid registration
Coordinate measuring machine
Micrometer precision

ABSTRACT

For the fabrication of dental inlays and crowns precise information on patients' teeth morphology is required. Besides the conventional method, where mold materials impressions are prepared, the use of digital scanners is more and more becoming a central part in the nowadays dentistry. The aim of the manuscript is to compare the accuracy of master models based on two intra-oral digital scanners and silicone impressions. A metal cast reference arch model with predefined measurement points was scanned using the Lava™ Chairside Oral Scanner C.O.S. and the iTero™ Intraoral Scanner respectively. These scans were applied for the fabrication of models using rapid prototyping and milling from a proprietary resin. In addition, plaster models were produced using conventional A-silicone impressions. Using a coordinate measuring machine and a micro computed tomography scanner the models were evaluated with micrometer precision. The mean distance deviations from model to model correspond to 112 μm (C.O.S.), 50 μm (iTero™) and 16 μm (gypsum). The results verified the high precision of the conventional technique based on A-silicone impressions and plaster models. The accuracy of the master models obtained on the basis of the digital scans is clinically sufficient to fabricate bridges with up to four units.

1. Introduction

The impression of teeth is an essential process step for manufacturing removable and fixed prosthodontics. Among other steps the clinical success depends on the precision of three-dimensional (3D) replica from the intraoral situation. The morphology of the prepared teeth is especially important, because the precision of the master model has direct impact on the fit of the restoration, e.g. the frame design or the veneering of a crown. A reasonable impression of an oral situation and the resulting master model is taking center stage of the prosthetic treatment [1]. The marginal, interdental, and intermaxillar fit of a prosthetic restoration is responsible for the clinical, long-term results [2]. A variety of impression materials were used during the last century. Sears introduced agar as an impression material for crowns in 1937 [3]. Thirty years later ESPE™ GmbH, Germany, introduced Impregum™, a polyether material. In 1975 A-silicones came onto the dental market. Twenty-five years later the Permadyne™-system altered the dentist's work [4]. Up to now, these impression materials are considered as gold standard. The first step in the prosthetic daily routine is to take an impression, e.g. using Alginate, before the fabrication of an individual tray on the plaster model. The individual tray is used to take an impression with materials such as polysiloxane, polyether or silicone with improved properties such as hydrophilicity, detail reproduction and shrinkage [5]. These impression materials result in accurate replicas of the prepared teeth and the periodontium [6,7]. The precision of the plaster models are influenced significantly by the processing aspects and impression technique [8]. The impression materials, however, are often suboptimal because of their flavor and the gagging reflex.

In 1980 digital prosthodontics entered the marketplace with the introduction of CEREC and in recent years digitizing takes more and more importance in dentistry [9,10]. Several production steps in the technician lab and in the dentist's surgery have a digital workflow, e.g. the frameworks of high-end full ceramic bridges (Y-TZP) CEREC, Straumann® CARES®, Guided Surgery. More and more manufacturers are offering devices for digital intra-oral impressions and computer-aided manufacturing (CAD/CAM). These attempts have the intention to automatize and simplify the procedure. The precision of the scanner-based replicas with respect to the

* Corresponding author.
E-mail address: georg.schulz@unibas.ch (G. Schulz).

http://dx.doi.org/10.1016/j.phmed.2016.04.002

conventional approaches, however, is hardly quantified. Pradies et al. [11] attested that impressions obtained from an intraoral digital scanner can be used in the normal clinical practice with better results than conventional impressions using elastomers. For serious discussions among dentists it is highly desirable to provide a direct and comprehensive comparison between the well-established impressions and the more recent digital intra-oral ones including the Lava™ Chairside Oral Scanner C.O.S. (3M™ ESPE™) and the iTero™ Intraoral Scanner (Straumann®). So far studies based on linear distance measurements are present [12,13] which assert the Lava™ Chairside Oral Scanner C.O.S. to be most precise compared to results obtained with the iTero™ Intraoral Scanner and the CEREC AC with CEREC Bluecam. Based on our clinical experience, we hypothesize that the two selected digital scanners provide impressions with a precision comparable to the gold standard. We further hypothesize that the more recently introduced digital approach has not fully reached the precision of the conventional impressions. It is the aim of the present study to quantitatively compare the precision of the results from the two procedures. To this end, not only selected distances are determined but also the mean and maximal deviations of the replica from the model are extracted with micrometer precision.

2. Materials and methods

2.1. Reference

A metallic cast, shaped in some way similar to a human jaw, served as dimensionally stable reference; see Fig. 1 (a). In the metal arch, which consists of chrome steel (type X5CrNi18-8), the human anatomy is only partially reflected. It contains simplifications with well-defined, characteristic features. These features enable the accurate measurement of pre-defined distances, as displayed in Fig. 2. Cylindrical holes 4 mm in diameter and 4 mm deep have been eroded into the tooth-representing structures, which might be termed 37, 38, 47, and 48, and are marked by red-colored circles in Fig. 2. The center of each cylinder coincides with the core area of the crown-like structure. The determination of the central points in the three-dimensional space with micrometer precision allows for the accurate measurements of distances between the crown-like features for the reference and the replicas.

2.2. Master models

Three methods were applied to produce master models from the reference cast. First, the cast was scanned for five times using the intra-oral scanner iTero™ Intraoral Scanner (Straumann Holding AG, Basel, Switzerland). Using these data, Cadent™ (Or Yehuda, Israel) fabricated master models by milling the proprietary resin [14]. Second, five digital impressions by means of the LAVA™ Chairside Oral Scanner (3M™ ESPE™ AG, Rüschlikon, Switzerland) were prepared. Here, the cast was sprayed using the titanium dioxide powder as recommended to improve the reflectivity properties within the oral cavity. The scans were performed according to the manufacturers' instructions. After sending the data to the processing center and transformation in an appropriate format the master model is produced by rapid prototyping [15]. Third, for the comparison with a conventional method, five impressions with A-silicone (Heraeus Flexitime® single step monophase, Heraeus Kulzer AG, Dübendorf, Switzerland) were taken in five individual trays. The five gypsum-models class IV (Fujirock®, GC Europe, Leuven, Belgium) were manufactured in the well-established

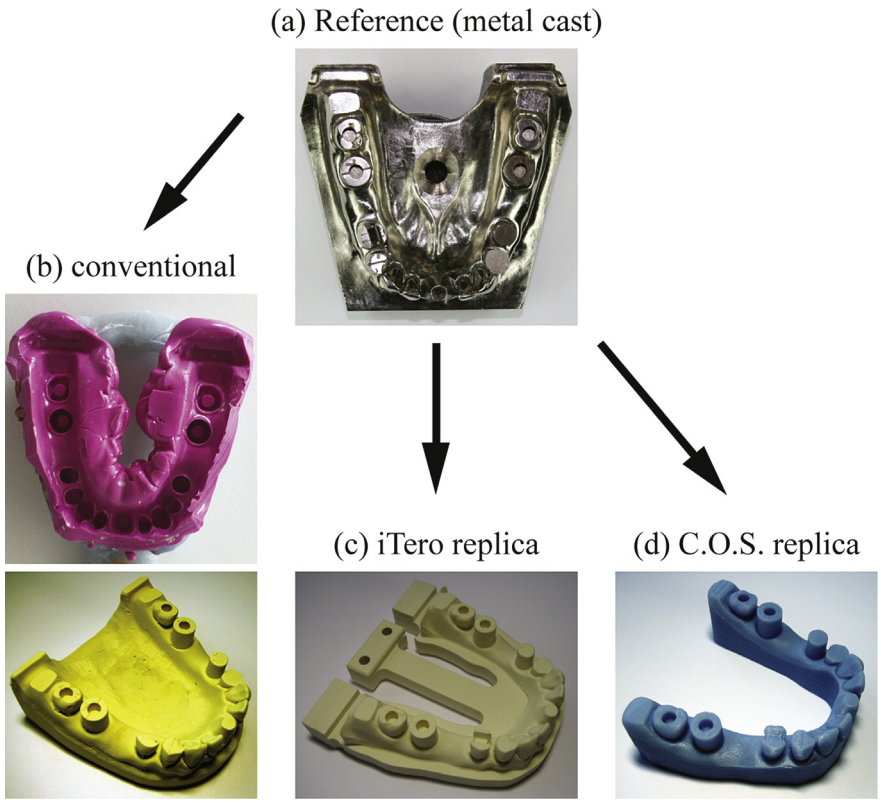

Fig. 1. The cast (a) served as reference for the replication in a conventional way via silicone and gypsum (b) and using the oral scanners iTero (c) and C.O.S. (d). The replication was performed for five times per technique, so that the dimensions and tolerances of the 15 replicas could quantitatively be compared with the physical dimensions of the metal reference.

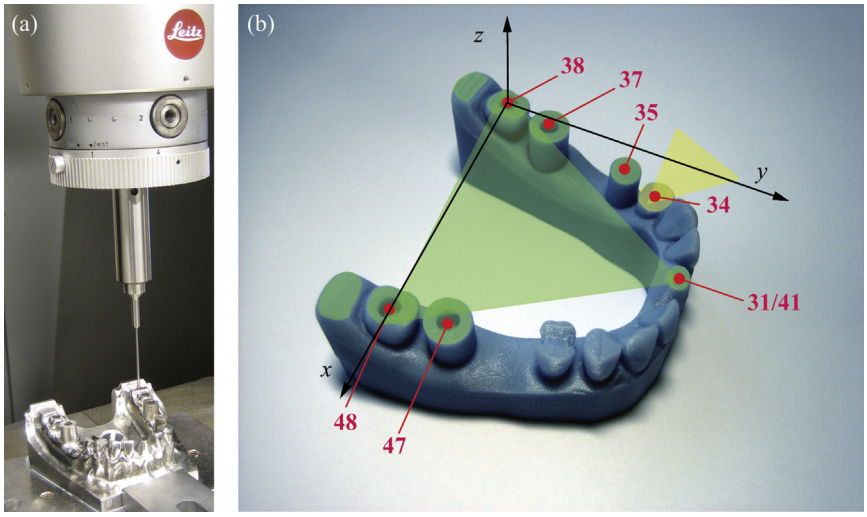

Fig. 2. The coordinate measuring machine (a) reaches micrometer precision in locating the features labeled 38, 37, 35, 34, 31/41, 47, and 48 (b) according to the pre-defined coordinate system. Besides the distances between the features, the physical dimensions of the cylinders from reference and replicas were determined.

manner.

2.3. Tactile coordinate measurements

Distance measurements with micrometer precision were performed using the coordinate measuring machine Leitz PMM 864 (Hexagon Metrology GmbH, Wetzlar, Germany). The coordinates of the points of interest were probed with a tactile sensor. At the end of this sensor a chromium-doped aluminum oxide sphere 2 mm in diameter was placed. The contact force applied corresponded to 20 mN. The software Quindos from Hexagon Metrology GmbH allowed for the control of the coordinate measuring machine. According to the ISO series 10360 [16] the maximum error for our length measurements is found to be 1.6 μm. The position of the eroded cylinders labeled by 38, 37, 48 and 47 as well as the cylinder labeled by 35 were measured 1 mm from the top plane, as indicated by the green-colored plane of Fig. 2. The coordinates of the center points were determined from 16 measurements per circle.

In order to reduce the uncertainties, the positions were measured incorporating a Monte-Carlo approach. The coordinates of each probing point were randomly selected from a uniform distribution with the error range given above. For each of the thousand runs, the positions of the best-fit circles through the simulated points were calculated.

The reference was measured four times, three times without changing the mounting and one time 90° rotated. These measurements affirmed the reproducibility of the measurements with deviations smaller than 0.6 μm and the independence of the 3D model orientation.

To evaluate and compare distances between the features of interest including the distance between 38 and 37, a coordinate system was introduced (cp. Fig. 2). The center points of the cylinders from the features 38 and 48 define the *x*-axis with the point of origin located at the center of feature 38. The *z*-direction arises from the normal of the plane, green-colored in Fig. 2, and is obtained from the best fit through the top surfaces of features labeled 38, 37, 35, 31/41, 47, and 48. The conventions of a Cartesian coordinate system yield the *y*-direction.

The coordinates measurements resulted in the three parameters, i.e. (i) the seven distances between the tooth-like features, (ii) the diameters of the four eroded cylinders and the one of feature 35, and (iii) the deviations of the eroded holes from the cylindrical shape.

2.4. Advanced micro computed tomography

The micro computed tomography (μCT) measurements were performed using the nanotom® m (phoenix|x-ray, GE Sensing & Inspection Technologies GmbH, Wunstorf, Germany) equipped with a 180 kV/15 W nanofocus® X-ray source. During the measurements the reference and the 15 replicas were fixed on the precision rotation stage. For each specimen a set of 1440 equiangular radiographs were taken over an angular range of 360°. For the cast (reference) an accelerating voltage of 180 kV and a beam current of 30 μA were used. For the scanning of the gypsum models an accelerating voltage of 150 kV and a beam current of 50 μA were adjusted, whereas for the scans of the iTero and the C.O.S. models an accelerating voltage of 80 kV and a beam current of 230 μA were applied. A 0.25 mm-thick Cu-filter was introduced to increase the mean photon energy. The exposure time for one radiograph was selected to 1.00 s for the cast, to 1.50 s for the iTero and C.O.S. replicas and to 0.75 s for the gypsum exemplars. After two-fold binning to improve the density resolution [17], the camera readout (3072 × 2400 pixels) resulted in a voxel length of 80 μm. The data were reconstructed taking advantage of the cone-beam filtered back-projection algorithm using phoenix datos|x 2.0 reconstruction version 2.0.1 – RTM (GE Sensing & Inspection Technologies GmbH).

The software VG Studio Max 2.0 (Volume Graphics, Heidelberg, Germany) served for the visualization of the three-dimensional data. Before registration, the specimens were segmented by an intensity-based approach [18]. These data were non-rigidly registered to localize dimensional changes between the 16 specimens as successfully applied previously [19–21]. The local differences between the replicas and the reference were quantified by means of the software Matlab 7.8 (Math works, Natick, USA).

3. Results

3.1. Distance measurements

Selected distances, i.e. between the features labeled 48–47, 38–35, 37–47, 38–37, 38–48, and 48–35, were determined using the coordinate measuring and the μCT system. Table 1 lists the

Table 1
The results of the distance measurements are given as mean values together with the standard deviations. Tactile measurements and μCT data are well comparable.

	Distance 48–47 [mm]	Distance 38–35 [mm]	Distance 37–47 [mm]	*z*-component [mm]
Reference	10.132[a]	28.214[a]	44.535[a]	0.843[a]
	10.111[b]	28.176[b]	44.488[b]	0.896[b]
Gypsum	10.140 ± 0.005[a]	28.230 ± 0.007[a]	44.556 ± 0.010[a]	0.846 ± 0.006[a]
	10.120 ± 0.008[b]	28.222 ± 0.040[b]	44.464 ± 0.009[b]	0.897 ± 0.025[b]
iTero	10.119 ± 0.011[a]	28.183 ± 0.053[a]	44.521 ± 0.084[a]	0.815 ± 0.038[a]
	10.106 ± 0.009[b]	28.228 ± 0.067[b]	44.570 ± 0.071[b]	0.790 ± 0.019[b]
C.O.S.	10.099 ± 0.051[a]	28.117 ± 0.168[a]	44.312 ± 0.268[a]	0.914 ± 0.048[a]
	10.104 ± 0.045[b]	28.142 ± 0.147[b]	44.340 ± 0.312[b]	0.947 ± 0.057[b]

	Distance 38–37 (mm)	Distance 38–48 (mm)	Distance 48–35 (mm)
Reference	10.301[a]	48.768[a]	50.214[a]
	10.304[b]	48.686[b]	50.138[b]
Gypsum	10.310 ± 0.003[a]	48.791 ± 0.010[a]	50.239 ± 0.014[a]
	10.289 ± 0.001[b]	48.687 ± 0.010[b]	50.161 ± 0.039[b]
iTero	10.282 ± 0.023[a]	48.699 ± 0.079[a]	50.130 ± 0.066[a]
	10.252 ± 0.049[b]	48.761 ± 0.069[b]	50.208 ± 0.052[b]
C.O.S.	10.283 ± 0.051[a]	48.438 ± 0.312[a]	49.994 ± 0.301[a]
	10.291 ± 0.047[b]	48.487 ± 0.378[b]	50.016 ± 0.308[b]

[a] Coordinate measuring machine.
[b] μCT.

mean values derived from the reference and the 15 replicas. For the iTero system a mean deviation of 66 μm was derived, whereas the conventional gypsum models exhibit a mean deviation as low as 19 μm. For the *y*-direction, the distances between the features 38–37, 38–35, and 48–47 show mean deviations of 34 μm (C.O.S. system), 29 μm (iTero system), and 17 μm (conventional approach using gypsum). Finally, the reproducibility in the *z*-direction was determined. Here, according to Fig. 2 the distance between the green-colored plane and the surface of feature 34 indicated by the yellow-colored plane in Fig. 2 was quantified. The C.O.S. system yielded a mean deviation of 61 μm, the iTero system 67 μm and the conventional gypsum-based approach 2 μm.

3.2. Diameter measurements

The cylindrical holes in the features labeled 38, 48, 37, and 47 have a nominal diameter of 4 mm. Feature 35 shows a circular shape on its surface with a nominal diameter of 6 mm (see Fig. 2). These five diameters were measured on the reference and the 15 replicas using the coordinate measuring machine. Table 2 summarizes the related data. Comparing the three approaches, we have found mean deviations of the replicas from the reference that correspond to 39 μm for C.O.S. system, 33 μm for iTero system, and 9 μm for the gypsum-based procedure.

3.3. Measured deviations from circular shapes

The five diameters considered in section 3.2 exhibit deviations from the perfect circular shape. These deviations are listed in Table 3. The mean values equal to 31 μm for the C.O.S. system, 51 μm for the iTero system and 6 μm for the gypsum-related, conventional technique.

3.4. Local displacement fields

The accuracy of fit can be best characterized using the local deviations in 3D space. To this end, the tomography data of the replicas were non-rigidly registered with the three-dimensional data from the reference [21]. As an example for each of the three fabrication routes Fig. 3 displays the local displacement fields by color-coded virtual arch models. The local deviations are color-coded as quantified by the color bar. The integral pixel displacements of the features labeled 38, 48, 37, 47 and 35 are given in Table 4.

4. Discussion

The precision of the distances extracted from the μCT measurements is surprising, as the voxel length after binning corresponds to 80 μm. Thus, one would expect a spatial resolution of about 120 μm. The distances, however, were calculated using more than 120 voxels per reference center, which increases the precision of the distance measurements drastically. It works, because the nanotom® m is designed for sub-micrometer resolution imaging and, therefore, provides the necessary mechanical stability. Furthermore, the supplier regularly calibrated the μCT-system during the yearly maintenance. Even more important, the imaging of the 15 models and the reference is a relative measurement, so that any systematic error is excluded. Still, one may doubt the precision of the results presented. The results of the independent recording using the coordinate measurement with the tactile sensors, however, prove the validity.

The deliverables of intensity-based segmentation of CT-data that are acquired with limited photon statistics often critically depend on the choice of the threshold [18]. In the present case, however, the determination of the center of the drilling is

Table 2
The diameters of five cylindrical holes of features with the labels 38, 48, 37, 47, and 35 measured with the coordinate measuring machine are given as mean values together with the standard deviations.

	38 [mm]	48 [mm]	37 [mm]	47 [mm]	35 [mm]
Reference	3.981	3.983	3.980	3.982	6.005
Gypsum	3.992 ± 0.003	3.992 ± 0.003	3.989 ± 0.004	3.990 ± 0.004	6.010 ± 0.014
iTero	3.949 ± 0.031	3.966 ± 0.016	3.917 ± 0.029	3.945 ± 0.033	5.991 ± 0.021
C.O.S.	3.938 ± 0.022	3.926 ± 0.014	3.948 ± 0.028	3.934 ± 0.022	6.019 ± 0.034

Table 3
Deviations of the four holes of features with the labels 38, 48, 37, 47, and cylinder 35 from cylindrical shape measured with the coordinate measuring machine are given as mean values together with the standard deviations.

	38 [mm]	48 [mm]	37 [mm]	47 [mm]	35 [mm]
Reference	0.010	0.009	0.014	0.007	0.002
Gypsum	0.010 ± 0.001	0.008 ± 0.004	0.013 ± 0.001	0.009 ± 0.003	0.027 ± 0.009
iTero	0.058 ± 0.021	0.047 ± 0.029	0.076 ± 0.008	0.057 ± 0.024	0.057 ± 0.027
C.O.S.	0.036 ± 0.011	0.047 ± 0.036	0.036 ± 0.011	0.035 ± 0.011	0.040 ± 0.017

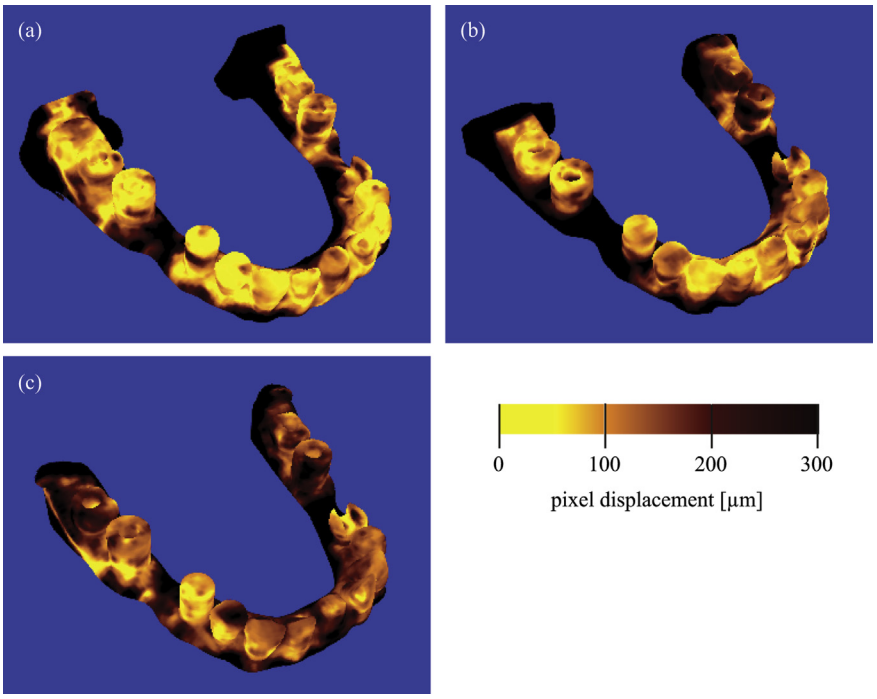

Fig. 3. The non-rigid, three-dimensional registration of the μCT data from the replicas with that of the reference allows for the localized quantification of the imperfections in replication. The images show the displacement fields of the conventional approach (a), the iTero scanning (b) and the C.O.S. system (c) with respect to the metal reference according to the color bar. (For interpretation of the references to colour in this figure legend, the reader is referred to the web version of this article.)

Table 4
Reproducibility of replication as characterized using the pixel displacements of the features labeled 38, 48, 37, 47 and 35 are given as mean values together with the standard deviations.

	38 [mm]	48 [mm]	37 [mm]	47 [mm]	35 [mm]
Gypsum	0.125 ± 0.073	0.117 ± 0.070	0.100 ± 0.055	0.118 ± 0.088	0.123 ± 0.056
iTero	0.202 ± 0.131	0.191 ± 0.121	0.224 ± 0.150	0.178 ± 0.093	0.150 ± 0.075
C.O.S.	0.212 ± 0.086.	0.192 ± 0.090	0.164 ± 0.062	0.223 ± 0.061	0.141 ± 0.070

insensitive to the choice of the threshold, especially also because the peaks for air and material within the histograms are well separated.

The fitting of dentures crucially depends on the micrometer replication of the necessary length scale. Imprecise dimensions can result in time-consuming finishing to be performed by the dentist. The quantification of the precision in fabricating dentures is vital to obtain argumentation means for the suitable comparison of the available procedures and to identify the potential for improvement. First, the distance measurements in section 3.1 give rise to values that are identical within a range much better than 100 μm. Second, the differences between the replicas and the reference are hardly detectable. Third, the repeatability characterized by means of the standard deviations is significantly smaller for the conventional gypsum compared to the two digital oral scanner approaches. Nevertheless, the reproducibility is high, since the error bars are smaller than 1%. Forth, the mean deviations for the distances between the replicas and the reference in the *x*-direction, related to the distances labeled 38–48, 37–47, and 35–48, were highest for the C.O.S. system and corresponded to 207 μm.

The use of a well defined standard instead the clinical situation in the oral cavity of patients has several disadvantages, but has to be regarded as *best scenario*, since in the clinical situation the accessibility is restricted by the limited mouth opening and possibly by an ascending ramus of the mandible. Further physiological circumstances including salivation and the sub-gingival preparation of teeth could hinder the dentist to take an accurate impression. If tissue hinders the view, optical scanners will not provide any reasonable sub-gingival impression.

Patients should not be confronted with a detailed comparison of the three techniques with seven teeth *in vivo*. The necessary procedures have even to be repeated in a random fashion to reach

statistical significance. Furthermore, the coordinate measuring machine cannot be applied to the oral cavity and *in vivo* measurements with high-resolution CT cannot be carried out because of the inacceptable X-ray dose.

Recent literature confirms that crowns produced by digital impression can have a better fit than crowns based on conventional impressions [22–24]. This observation is easily understood, as the crown framework directly designed from the intra-oral data is milled from solid ceramic materials. One can omit the manufacture of a master model and eliminates the need for a gypsum model. The smaller marginal gap of crown's frames is the main advantage of the digital workflow, although the technician has to veneer the framework for aesthetic reasons. Master models serve for the space control to the neighboring teeth and arches, respectively. The dimensional accuracy is responsible for the clinically relevant interproximal contact and the occlusion of the fixed prosthetic work [2]. The physiological tooth mobility of 30–100 μm gives certain flexibility in mesial and distal directions [25,26]. Therefore, such deviations are clinically tolerable. Thus, the mean deviations of 16 μm (C.O.S.), 36 μm (iTero) and 12 μm (gypsum) between feature 37 and 38 as well as of 20 μm (C.O.S.), 9 μm (iTero) and 8 μm (gypsum) between features 47 and 48 are acceptable. Even for distances that correspond to a four-unit bridge and the spacing between features 38 and 35 the measured mean deviations of 65 μm for C.O.S., 41 μm for iTero, and 31 μm for gypsum were well below the limit of 100 μm.

Fixed prosthetic works in dentist's daily routine are most frequently single crowns or bridges in a sextant. For these reconstructions the deviation in the *y*-direction is relevant. Syrek et al. [22] attested a better fit of single crowns in a posterior molar resulting from intra-oral scans. In the present study, we replicated best feature 35, which equates in some respects a single unit crown. The mean deviations of the diameter were 14 μm (C.O.S.), 14 μm (iTero), and 5 μm (gypsum). The mean deviations in *x*- and *z*-directions were larger. Recent literature and our practical experience indicate that intra-oral impressions could fail in the superimposition of the frontal region, because the models show compression in the molar regions [27]. The present communication reports differences for the distance measured between the features 38–48 and 35–48, which generally cannot be tolerated especially for the C.O.S. system, as they clearly exceed 100 μm. Here, the arch models are compressed in *x*-direction. Such distances equal full arch bridges. Since currently the framework size of the LAVA™ zirconia does not exceed a size of 60 mm, the precision is reasonably accurate.

Most distances measured on the gypsum models were larger than the ones of the metal reference. This volume expansion of the gypsum data is expected for Flexitime monophase and gypsum Fujirock. Piwowarcyk et al. [6] demonstrated that Flexitime monophase has a maximal contraction of 0.04% and the gypsum Fujirock an expansion of about 0.08% [28]. Results similar to the present study were shown by Caputi et al. [23]. In their work on the accuracy of monophase impressions from a steel standard they demonstrated that the dimensions on the gypsum (Fujirock) model were larger than the corresponding dimensions on the steel standard.

Although the distances in *z*-direction showed larger discrepancies for the optical scanner systems, it does not mean that prosthetic restorations of digital workflow have worse occlusal contact than of the conventional impression method. The conventional method relies on bite registration masses. These polymers are between lower and upper jaw and can hamper the registration for perfect occlusion. During the digital workflow the dentist takes the bite registration in central occlusion without any mass. Consequently, the occlusal behavior of digitally produced crowns is described as clinically sufficient [22,29].

In addition to the linear measurements listed in Tables 1–3, the three-dimensional μCT-data allow for quantifying local deviations of the master models from the reference. Such quantification is reproduced in the images of Fig. 3 using a color code. The values in Table 4 for the digital scanner systems are equal, whereas the conventional approach leads to slightly improved results. It is obvious that the oral scanners do not reach the quality of the conventional approach, but for bridges with up to four units the precision is clinically sufficient. The compression of the scanner-based models in transversal direction may arise from the superimposition in frontal region during the scan and a distortion of the master models during the production procedure. These transversal compressions of the models would have only a significant influence on full arch prosthetic reconstruction including full arch bridges and removable prosthodontics such as telescope crowns.

5. Conclusions

Digital impressions can be regarded as a paradigm shift in the present and future prosthetic dentistry. The digital workflow will become more and more important. The related models that are used for the veneering of frameworks for fixed prosthetic restorations are clinically sufficient to reproduce the oral situation for sizes up to a four-unit bridge. Several studies have proven the better fit of digitally designed frameworks. The main source of improvement lies in the model production of full arch bridges. It is only a matter of time till the master models will be as precise as the scan data itself.

Acknowledgements

The authors thank Emil Mangold AG, Oberdorf, Switzerland for the realization of the reference. The companies Straumann® AG, Basel, Switzerland, 3M™ ESPE™ AG, Rüschlikon, Switzerland and Zahntechnik Ess, Olten, Switzerland kindly produced the master models. The authors gratefully acknowledge T. Liebrich and S. Weikert (IWF / inspire AG, ETH Zurich) for the tactile coordinate measurements. The financial support of the Swiss National Science Foundation in the frame of the R'Equip initiative (project number 316030_133802) is gratefully acknowledged.

References

[1] J. Wirz, K. Jäger, F. Schmidli, Abformung in der zahnärztlichen Praxis, Elsevier, München, 1993.
[2] P. Pospiech, Chipping - systemimmanente oder verarbeitungsbedingte Probleme? Quintessenz 61 (2010) 173–181.
[3] A.W. Sears, Hydrocolloid impression technique for inlays and fixed bridges, Dent. Dig. 43 (1937) 230–234.
[4] W. Brücking, Die perfekte Abformung, Quintessenz 57 (2006) 59–75.
[5] T.E. Donovan, W.W. Chee, A review of contemporary impression materials and techniques, Dent. Clin. North Am. 48 (2004) 445–470.
[6] A. Piwowarczyk, P. Ottl, A. Büchler, H.C. Lauer, A. Hoffmann, In vitro study on the dimensional accuracy of selected materials for monophase elastic impression making, Int. J. Prosthodont 15 (2002) 168–174.
[7] D. Papadogiannis, R. Lakes, D. Palaghias, Y. Papadogiannis, Effect of storage time on the viscoelastic properties of elastomeric impression materials, J. Prosthodont. Res. 56 (2012) 11–18.
[8] H. Rudolph, M.R.S. Graf, K. Kuhn, S. Rupf-Köhler, A. Eirich, C. Edelmann, et al., Performance of dental impression materials: benchmarking of materials and techniques by three-dimensional analysis, Dent. Mater. J. 34 (2015) 572–584, http://dx.doi.org/10.4012/dmj.2014-197.
[9] W. Mörmann, The evolution of the CEREC system, J. Am. Dent. Assoc. 137 (Suppl) (2006) 7S–13S.
[10] P. Kachalia, M.J. Geissberger, Dentistry a la carte: in-office CAD/CAM technology, J. Calif. Dent. Assoc. 38 (2010) 323–330.
[11] G. Pradies, C. Zarauz, A. Valverde, A. Ferreiroa, F. Martínez-Rus, Clinical evaluation comparing the fit of all-ceramic crowns obtained from silicone and digital intraoral impressions based on wavefront sampling technology, J. Dent. 43 (2015) 201–208.

[12] W.J. van der Meer, F.S. Andriessen, D. Wismeijer, Y. Ren, Application of intra-oral dental scanners in the digital workflow of implantology, PLoS One 7 (2012) e43312, http://dx.doi.org/10.1371/journal.pone.0043312.
[13] A. Ender, A. Mehl, Influence of scanning strategies on the accuracy of digital intraoral scanning systems, Int. J. Comput. Dent. 16 (2013) 11–21.
[14] A.K. Garg, Cadent iTero's digital system for dental impressions: the end of trays and putty? Dent. Implantol. Update 19 (2008) 9–11.
[15] K. Jäger, C. Vögtlin, Digitaler Workflow mit dem Lava Chairside Oral Scanner C. O. S und der Lava-Technik, Schweiz. Monatsschrift Für Zahnmed. 122 (2012) 307–315.
[16] Geometrical ISO, Product Specifications (GPS) - Acceptance and Reverification Tests for Coordinate Measuring Machines (CMM), Switzerland, Geneva, 2000.
[17] P. Thurner, F. Beckmann, B. Müller, An optimization procedure for spatial and density resolution in hard X-ray micro-computed tomography, Nucl. Instrum. Methods Phys. Res. Sect. B 225 (2004) 599–603.
[18] B. Müller, F. Beckmann, M. Huser, F. Maspero, G. Székely, K. Ruffieux, et al., Non-destructive three-dimensional evaluation of a polymer sponge by micro-tomography using synchrotron radiation, Biomol. Eng. 19 (2002) 73–78.
[19] M. Germann, A. Morel, F. Beckmann, A. Andronache, D. Jeanmonod, B. Müller, Strain fields in histological slices of brain tissue determined by synchrotron radiation-based micro computed tomography, J. Neurosci. Methods 170 (2008) 149–155.
[20] G. Schulz, H.J. Crooijmans, M. Germann, K. Scheffler, M. Müller-Gerbl, B. Müller, Threedimensional strain fields in human brain resulting from formalin fixation, J. Neurosci. Methods 202 (2011) 17–27.
[21] B. Müller, H. Deyhle, S. Lang, G. Schulz, T. Bormann, F. Fierz, et al., Three-dimensional registration of tomography data for quantification in bio-materials science, Int. J. Mater. Res. 103 (2012) 242–249.
[22] A. Syrek, G. Reich, D. Ranftl, C. Klein, B. Cerny, J. Brodesser, Clinical evaluation of all ceramic crowns fabricated from intraoral impressions based on the principle of active wavefront sampling, J. Dent. 38 (2010) 553–559.
[23] S. Caputi, G. Varvara, Dimensional accuracy of resultant casts made by a monophase, one-step and two-step, and a novel two-step putty/light-body impression technique: an in vitro study, J. Prosthet. Dent. 99 (2008) 274–281.
[24] A. Ender, A. Mehl, Full arch scans: conventional versus digital impressions - an in vitro study, Int. J. Comput. Dent. 14 (2011) 11–21.
[25] R. Ott, H.P. Vollmer, W. Krug, Klinik- und Praxisführer Zahnmedizin, Thieme, Stuttgart, 2002.
[26] P. Castellini, L. Scalise, E.P. Tomasini, Teeth mobility measurement: a laser vibrometry approach, J. Clin. Laser Med. Surg. 16 (1998) 269–272.
[27] T. Vauthier, R. Jung, S. Paul, F. Paqué, A. Mehl, C. Katsaros, et al., Vom Bohrer zur Maus, Schweiz. Monatsschrift Für Zahnmed. 121 (2011) 1206–1210.
[28] GC, Three First Class Type 4 Dental Die Stones: All-purpose, Free-flowing or CAD/CAMoptimised, n.d, 2009. www.gceurope.com/news/press/200903/en_fujirock.doc.
[29] R. Scotti, P. Cardelli, P. Baldissara, C. Monaco, Clinical fitting of CAD/CAM zirconia single crowns generated from digital intraoral impressions based on active wavefront sampling, J. Dent. (2011), http://dx.doi.org/10.1016/j.jdent.2011.10.005.